Minimal Model of Oscillations and Waves in the *Limax* Olfactory Lobe With Tests of the Model's Predictive Power

BARD ERMENTROUT,[1] JORGE FLORES,[2] AND ALAN GELPERIN[2]
[1]*Department of Mathematics, University of Pittsburgh, Pittsburgh, Pennsylvania 15260; and* [2]*Biological Computation Research Department, Bell Laboratories, Lucent Technologies, Murray Hill, New Jersey 07974*

Ermentrout, Bard, Jorge Flores, and Alan Gelperin. Minimal model of oscillations and waves in the *Limax* olfactory lobe with tests of the model's predictive power. *J. Neurophysiol.* 79: 2677–2689, 1998. Propagating waves are observed in the olfactory or procerebral (PC) lobe of the terrestrial mollusk, *Limax maximus*. Wave propagation is altered by cutting through the various layers of the PC lobe both parallel and transverse to the direction of wave propagation. We present a model for the PC lobe based on two layers of coupled cells. The top layer represents the cell layer of the PC lobe, and the bottom layer corresponds to the neuropil of the PC lobe. To get wave propagation, we induce a coupling gradient so that the most apical cells receive a greater input from neighbors than the basal cells. The top layer in the model is composed of oscillators coupled locally, whereas the bottom layer is comprised of oscillators with global coupling. Odor stimulation is represented by an increase in the strength of coupling between the two layers. This model allows us to explain a number of experimental observations: *1*) the intact PC lobe exhibits regular propagating waves, which travel from the apical to the basal end; *2*) there is a gradient in the local frequency of slices cut transverse to the axis of wave propagation, with apical slices oscillating faster than basal slices; *3*) with partial cuts through the cell layer or the neuropil layer, the apical and basal ends remain tightly coupled; *4*) removal of the neuropil layer does not prevent wave propagation in the cell layer; *5*) odor stimulation causes the waves to collapse and the cells in the PC lobe oscillate synchronously; and *6*) by allowing a single parameter to vary in the model, we capture the reversal of waves in low chloride medium.

INTRODUCTION

Central circuits processing olfactory information display spontaneous or stimulus-induced oscillations in a large number of species (Adrian 1942; Gelperin and Tank 1990; Gray 1994; Tank et al. 1994). A variety of alternative proposals for the role of olfactory oscillations in odor recognition or categorization have been made (Gelperin et al. 1996; Hopfield 1995; Laurent et al. 1996; Wehr and Laurent 1996). Recent results from honeybee suggest that coherent oscillations in central olfactory centers may be required for discrimination of closely related odors (Stopfer et al. 1997). The ubiquitous nature of coherent oscillations in olfactory bulb and its analogous structures in invertebrates suggests that olfactory oscillations may have a computational function of wide generality.

Wave-like propagation of activity through central neural structures has been observed in mammalian brain and the mollusk *Limax maximus*. In ferret thalamic slices, spindle oscillations consistently propagate in the dorsal-ventral axis (Kim et al. 1995). A modeling study by Golomb et al. (1996) clarified the factors that influence the propagation of activity in the thalamic reticular nucleus. With magnetoencephalography, a fronto-occipital phase shift of 12–13 ms was found for 40-Hz oscillatory activity in normal human subjects during wakefulness and during rapid-eye–movement sleep states (Llinas and Ribary 1993). The olfactory lobe of the terrestrial mollusk *L. maximus* shows wave-like propagation of activity that is modulated by odor stimulation (Delaney et al. 1994; Gervais et al. 1996; Kleinfeld et al. 1994).

There are many detailed biophysical models of cells that are capable of producing regular period bursts or spikes either due to intrinsic properties or through local network interactions (Gray and McCormick 1996; Traub et al. 1997). At the other extreme, one can model each neuron by a single dynamic variable. Integrate and fire neurons (van Vreeswijk et al. 1994) are one example of this. Indeed, there have been a number of studies of how integrate and fire neurons behave when coupled together into networks (van Vreeswijk et al. 1994). However, the synaptic coupling of this type of neuron in a model for the procerebral (PC) lobe is unknown. Another type of simplified model assumes each oscillating cell or circuit can be represented by a single variable, the phase. Then coupling between cells is manifested by a periodic function of the phase difference between the two oscillators (see Kopell and Ermentrout 1988). Because the membrane properties of the cells that generate the oscillations in the PC lobe are virtually unknown as are the connectivities between cells, we will adapt this more abstract approach. Such models have the advantage that they ''predict'' exactly the types of quantities that can be measured experimentally, namely phase lags between different regions of the PC lobe. Furthermore, certain emergent properties occur in groups of coupled oscillators that depend on very general properties of the interactions between cells. Phase models can be derived quantitatively from ''more realistic'' biophysical models of neurons, so that until a full membrane model is developed for PC lobe cells, the phase model description should be satisfactory.

METHODS

Specimens of *L. maximus* were obtained from a laboratory colony maintained on a 14:10 h light:dark cycle at 16°C with ad libitum access to lab chow (Purina) supplemented with vitamins, sea sand, and the fungicide Tegosept. Slugs were chilled to 4°C, and the brain and buccal mass quickly isolated into saline previously chilled to 4°C. The PC lobe was isolated from the cerebral ganglion by fine dissection.

0022-3077/98 $5.00

Sections of the PC lobe were made by embedding the desheathed lobe in 2.0% agarose in saline at 39°C. The tissue was sectioned at room temperature with 5 mg/ml bovine serum albumin added to the saline bathing the tissue block. Sections could be cut as thin as 50 μm, however, reliable oscillations were obtained from sections $\geq$125 μm. By orienting the tissue in the agar and trimming the agar block before cutting, sections could be obtained normal to or along the apical-basal axis of wave propagation. Sections were collected from the saline-filled well of the Vibratome, transferred to a silicone elastomer (Sylgard)-lined recording chamber and fixed to the Sylgard substrate by pins through the agar surrounding the tissue.

Recordings of local field potential (LFP) at one or two sites were made using saline-filled patch electrodes with 2- to 3-μm tip opening ($R \leq 1$ MΩ) placed in the cell body layer of the PC lobe slice. Current-to-voltage conversion was obtained with a patch-clamp amplifier (List EPC-7) operated in voltage-clamp search mode and low-pass filtered at 30 Hz (PAR model 113). Signals were digitized at 200 Hz and stored on a computer (Mac IIfx). Custom software controlled data acquisition and display. A commercial software package (Igor Pro) was used for data analysis.

Simulations of dynamical equations were made using custom software (XPP or XTC, available at http://www3.pitt.edu/~phase/) running on a UNIX workstation. The output of the model was taken either as the spatial pattern of activity over the array of units or as the simulated voltage of individual units.

RESULTS

Intact PC lobe

PHYSIOLOGY. The PC lobe is composed of two distinct regions of neuropil and a layer of neuronal somata. These three regions of the PC are seen clearly in a stained 200-μm–thick longitudinal section of an agar-embedded lobe cut along the apical-basal axis (Fig. 1*A*). The neuropil layer adjacent to the cell body layer is the terminal mass (TM), whereas the basal neuropil layer is the inner mass (IM) (Zaitseva 1991; Zs.-Nagy and Sakharov 1970). The cell body layer is thickest at the apex and thins progressively toward the base of the PC. Scattered cells are evident in the neuropil regions. The cell and neuropil regions are also evident in a transverse section cut across the apical-basal axis (Fig. 1*B*). The relative volumes of cell layer to neuropil and TM to IM vary in transverse sections taken from apical or basal regions of the PC.

The intact PC lobe shows waves of activity originating at the apical pole and propagating at 1.1 mm/s to the basal pole (Kleinfeld et al. 1994). With a typical apical-basal length of 700 μm for a 10-g slug and wave repetition rate of 0.7 Hz (Gelperin et al. 1993), only a single wave propagates and the duty cycle for wave propagation is $\sim$0.45. A distributed network of coupled burster (B) neurons drives the oscillation in LFP, which arises from extracellular currents driven by the coherent inhibitory postsynaptic potentials produced in nonbursting (NB) cells by B cell activity (Kleinfeld et al. 1994). The B cells have their somata, and all their neurites and synapses in the cell layer of the PC (Watanabe et al. 1997). In contrast, the NB cells have somata in the cell layer but their extensively branched neurites and synaptic connections are in the neuropil layer (Ratte and Chase 1997). On this basis, we take interactions in the cell layer to be dominated by B cell-B cell interactions, whereas the interactions in the neuropil layer are dominated by NB cell-NB cell interactions and input-NB cell interactions (Kawahara et al. 1997). The interactions between B cells and NB cells in the PC lobe occur at or near the interface between the cell and neuropil layers.

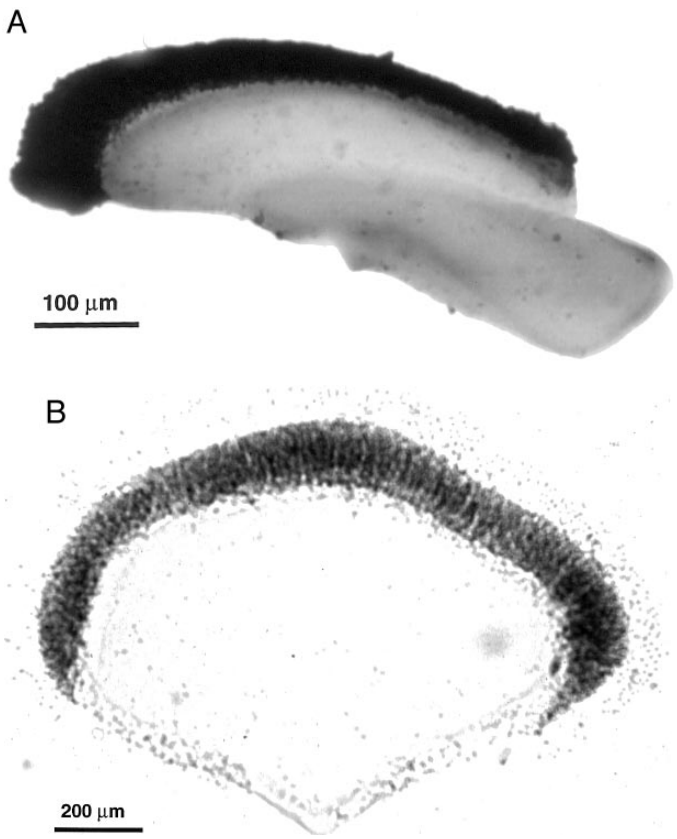

FIG. 1. Sections of procerebral lobes embedded in agarose and stained with toluidine blue. *A*: longitudinal 200-μm-thick section cut along the apical-basal axis of wave propagation. Cell body layer and 2 neuropil regions are evident. *B*: transverse 200-μm-thick section from the midregion of the procerebral (PC) lobe cut across the apical-basal axis of wave propagation. Staining as in *A*. Scale bar = 100 μm.

MODEL. There are many mechanisms by which propagating oscillatory waves can be produced. The simplest is to assume that the tissue is at rest and that there is a localized region of increased excitation that acts as a pacemaker. This simple mechanism can be eliminated for the PC lobe since small pieces (0.1 of PC) taken from various regions of the cell body layer continue to oscillate (Kleinfeld et al. 1994). This suggests that the oscillations are generated by intrinsically oscillatory cells (B cells) or local networks of B cells; this motivates our model. The isolated apical half of the PC oscillates faster than the basal half, suggesting that there is a gradient in the inherent frequency of B cells. The PC lobe has a gradient in thickness from apex to base so that if B cells in the thicker apical region have more synaptic inputs than B cells at the base, a frequency gradient is produced.

We have two types of cells in the model. One represents the locally connected B cells, and the other represents the NB cells. We assume that the NB cells are like B cells but normally are too hyperpolarized to burst. The connections between B cells are considered to be local in space. The NB cells are thought to be associated with odor recognition, and thus there is no spatial organization in their coupling. We

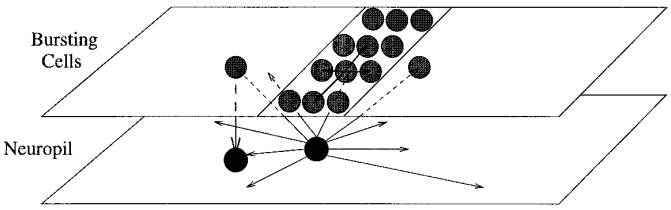

FIG. 2. Geometry of the model PC lobe. There are 2 layers to the model: top layer consists of locally coupled bursting cells and lower layer consists of globally coupled interneurons.

assume that the majority of NB cells make their synapses in the neuropil rather than the cell layer. Because we have assumed no spatial organization between the NB cells, we let the coupling between them be global in extent. Figure 2 shows a schematic of the model, represented as two layers, but this is only for illustration; B and NB cells both lie in the cell layer. The role of the neuropil in our model is that it is where the global coupling of the NB cells is proposed to occur. The model consists of the following:

1) A population of coupled B cells with coupling strength decreasing along the apical-basal axis to account for the increased cell number at the apical end. If cells in a local region are synchronized as we assume, then the larger the number of cells, the greater the interactions between them. This is the rationale for our assumption of a coupling gradient. The gradient in coupling strength is effectively the same as imposing an intrinsic frequency gradient. Lowering the effective frequency gradient (by for example lowering the coupling strength gradient) will cause the phase gradient to also be reduced. Synapses between B cells occur in the cell layer.

2) A population of NB cells. As we noted above, these are globally coupled with synapses that occur in the neuropil. (In fact, we do not require strictly global coupling. We can get by with random coupling between NB cells as long as the coupling between any 2 cells does not depend on distance between them.) The NB cells receive spatially local synapses from B cells and send out global or at least nonspatially organized synapses to B cells.

3) Each cell is represented by a single phase variable and thus corresponds to an oscillator. Coupling between cells is modeled as a periodic function of the phase-difference between the cells. Inactive NB cells (in absence of odorant stimuli) do not contribute to the coupling.

4) Odorant stimuli increase the activity of the NB cells. This activation is likely to be very specific to different odors. However, we assume that the spatial pattern of activity is not organized in a distance dependent fashion and thus the increase in activity is spatially distributed. The effect of increased activity is manifested in the model as an increase in the amount of input to the B cells from the NB cells.

The model for the bursting cells consists of the following phase equations

$$\frac{d\theta_{ij}}{dt} = \omega_0 + \sum_{nnbs} A_i H_{bb}(\omega_{i'j'} - \theta_{ij}) \quad (1)$$

$$+S(t) \sum_{i'j'} H_{nb}(\phi_{i'j'} - \theta_{ij}) \quad (2)$$

Here θ_{ij} is the phase of a B cell at position (i, j) and ϕ_{ij} is the phase of a NB cell. The index i corresponds to the proximal-distal axis, and the index j to the transverse direction. The first sum is over B cell nearest neighbors and the second over all NB cells. The amplitude of the local synaptic interaction is given by A_i. We assume that A_i is a decreasing function corresponding to the decreasing number of synapses onto B cells along the apical-basal axis. The function $S(t)$ is small and positive when there is no odorant and increases when odorant is applied. This effectively increases the interaction strength of the NB cells to the B cells, reflecting the recruitment of the NB cells during stimulation. In the absence of any interactions, all B cells fire at roughly the same frequency, ω_0. We imposed a frequency gradient through the coupling term (A_i) but obtained the same results with a gradient in intrinsic frequency, $\omega = \omega_i$.

The functions H represent the interactions between B cells and NB cells. For a specific model, they can be computed numerically. They are periodic functions of the phase difference between two oscillators. In the absence of inhomogeneities, we want two mutually coupled cells to synchronize, thus, we want the functions H to have a positive slope at zero phase difference (Ermentrout and Kopell 1991, 1994). We also assume that the functions H are roughly sinusoidal in shape, by which we mean that they have one local maximum and one local minimum per cycle. There are many mechanisms of coupling between cells that can give rise to interaction functions that have these properties. For example, excitatory synapses between the Hodgkin-Huxley membrane model or inhibitory interactions between cells that have the Traub sodium-delayed rectifier dynamics will both give interaction functions with this property (Hansel et al. 1995). This is why we want to avoid the use of specific models; there are many different ways to get the same results.

The most general form for the NB cells is

$$\frac{d\phi_{ij}}{dt} = \omega 0 + H_{bn}(\theta_{ij} - \phi_{ij}) + \sum_{i'j'} H_{nn}(\phi_{i'j'} - \phi_{ij}) \quad (3)$$

To simplify the numerical simulations and speed up computations, we assume that the NB cell at a spatial point (i, j) is locked tightly to the B cell at that point. This allows us to replace the phase of the NB cell, ϕ_{ij} with that of its neighboring B cell, θ_{ij} in the preceding equations. We have done some of the simulations maintaining the equations for the NB cells and found no more than a slight quantitative difference.

We have assumed that the interaction functions were ''sinusoidal'' in shape, and this form has been shown to occur in averaged behavior of biophysical models (Ermentrout and Kopell 1991; Hansel et al. 1995). Thus we take the interaction functions to be of the form

$$H(\theta) = C + K \sin(\theta - \xi) \quad (4)$$

where C, K, and ξ are constants. We choose $\xi < 0$ and $C \geq 0$ so that the effect of coupling between cells raises their frequency. Thus cells with more coupling connections oscillate faster and waves will originate at the point with the most coupling synapses, namely, at the apex of the PC lobe. The choice of $K > 0$ guarantees stability of the local waves. With these simplifications, we have run simulations with $\phi_{ij} = \theta_{ij}$. The simulations consist of four rows of 20 cells

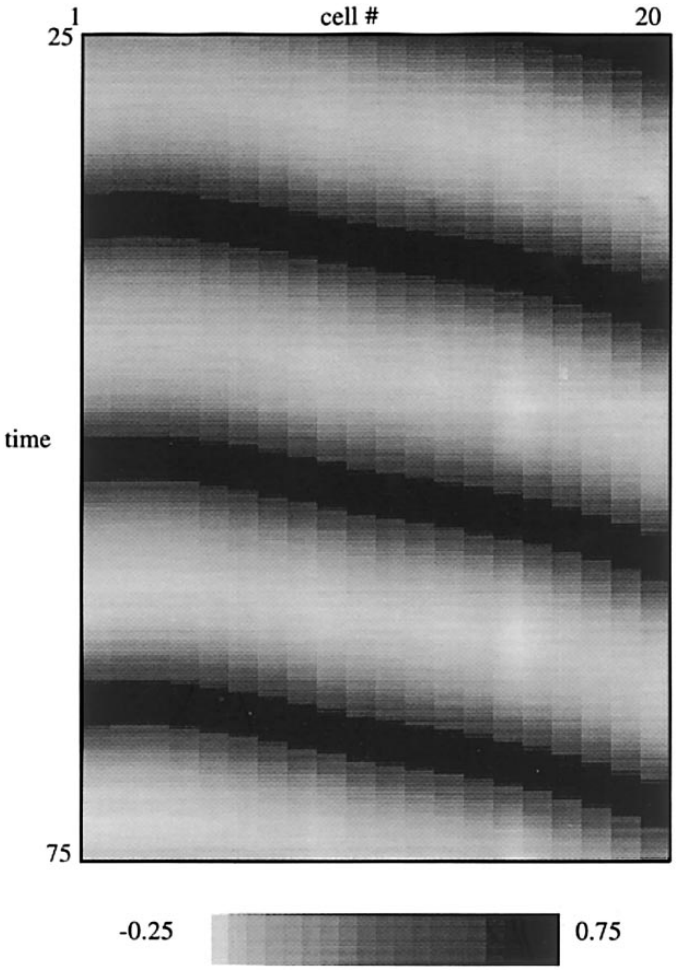

FIG. 3. Pseudopotentials of the phases for the model in the normal unstimulated, uncut preparation. Parameters are $C = 0$, $K = 1$, $\xi = -0.1$ for the interaction between local bursting cells; $C = 0$, $K = 0.05$, $\xi = -0.1$ for the neuropil bursting interaction; $\omega_0 = 0.15$, the base uncoupled frequency; $\epsilon = 0.008$, the unstimulated feedback of the neuropil to the bursting cells; and $Ai = 1 - 0.03i$, the coupling gradient. Time scales are in arbitrary units as only the relative times matter. Pseudopotentials are obtained by applying the function $V(\theta) = \exp[-12(1 + \cos\theta)] - 0.25$ to the phases. This function has a maximum peak of 0.75 at $\theta = \pi$ and a minimum of $\sim$0.25 at $\theta = 0$. Because phase models provide information about phase, the choice of amplitude is arbitrary.

coupled to nearest neighbors via the function H_{bb} and globally coupled via the function H_{nb}. Parameters are given in the figure legends.

The normal behavior of the model is to generate traveling periodic waves resulting in a phase-gradient along the apical-basal axis (Fig. 3). The magnitude of the total phase gradient depends on the parameters chosen for the interaction functions, in particular ξ and C. The total lag along the apical-basal axis of the lobe is roughly one period of the oscillation. This suggests that there may be some global coupling that could set this lag (e.g., local synchronizing coupling with global antiphasic coupling) (see Ermentrout and Kopell 1994). However the phase lag appears on cut slices in which global coupling would be disrupted. This, together with the evident gradient in intrinsic frequency (see further), leads us to suggest that the total gradient may be more variable and is not globally controlled. However, we believe that there is global synchronizing coupling when an odor stimulus is presented.

Slices cut across wave axis

PHYSIOLOGY. The oscillation frequencies of a series of 150-μm−thick transverse slices cut normal to the apical-basal axis of wave propagation are shown in Fig. 4*A*. The most apical slice had the highest oscillation frequency, whereas the most basal slice had the lowest frequency. The slice frequencies cover a range spanning the 0.7-Hz frequency of the intact PC lobe. The transverse slices still propagate apical-basal waves as seen in the nonzero offset of the first peak in the cross-correlation between the field potential recordings obtained from apical and basal sites within a slice (Fig. 4*B*).

MODEL. In Fig. 4*C*, we show the behavior of both halves of the model after the model is cut in half between rows 10 and 11. The phase lag is maintained within each half and the apical slice (left) has the higher frequency. When the model is cut into five transverse slices, the oscillation frequencies increase monotonically from apex to base (Fig. 4*D*), as did the slices from the PC lobe.

Slices cut along wave axis

PHYSIOLOGY. Longitudinal slices of the PC lobe cut along the apical-basal axis propagate a wave from apex to base as shown by phase delays between peak activity at apical and basal recording sites, reflected in the nonzero offset of the cross-correlation between apical and basal recordings (Fig. 5*A*). The electrode spacing was 600 μm for the data in Fig. 5*A*, with a temporal offset of 550 ms, corresponding to a wave velocity of 1.1 mm/s. This is in good agreement with the value obtained for intact PC lobes measured optically (Kleinfeld et al. 1994). The oscillation frequency of the slice in Fig. 5*A* is 0.7 Hz. Some longitudinal slices show periods of wave activity interrupted by rapid transitions from wave propagation to spatially uniform activity and return to wave propagation (Fig. 5*B*). The activity wave in the longitudinal slice propagates uniformly through the cell and neuropil layers, as determined from analysis of a digitized image series of slices stained with the voltage sensitive dye di-4-ANEPPS (No. D-1199, Molecular Probes, Eugene, OR; data not shown).

MODEL. We have simulated longitudinal slices, and there is little difference from the intact preparation. The simulation of the slice experiments involves simply disconnecting the rows of 20 cells from neighboring rows by setting the coupling between rows to 0. We do not see bouts of spatially uniform activity in the model; we assume this is due to noise, inhomogeneities, or other perturbations absent in the model but present in PC tissue. The main difference is that the frequency is lowered by 60% and the phase gradient is larger. The lowering of the frequency is expected since the effect of coupling is to increase the activity and thus the burst frequency of the cells.

Activity after cutting cell layer

PHYSIOLOGY. Because the isolated cell body layer can oscillate and propagate apical-basal waves, we assumed that cutting com-

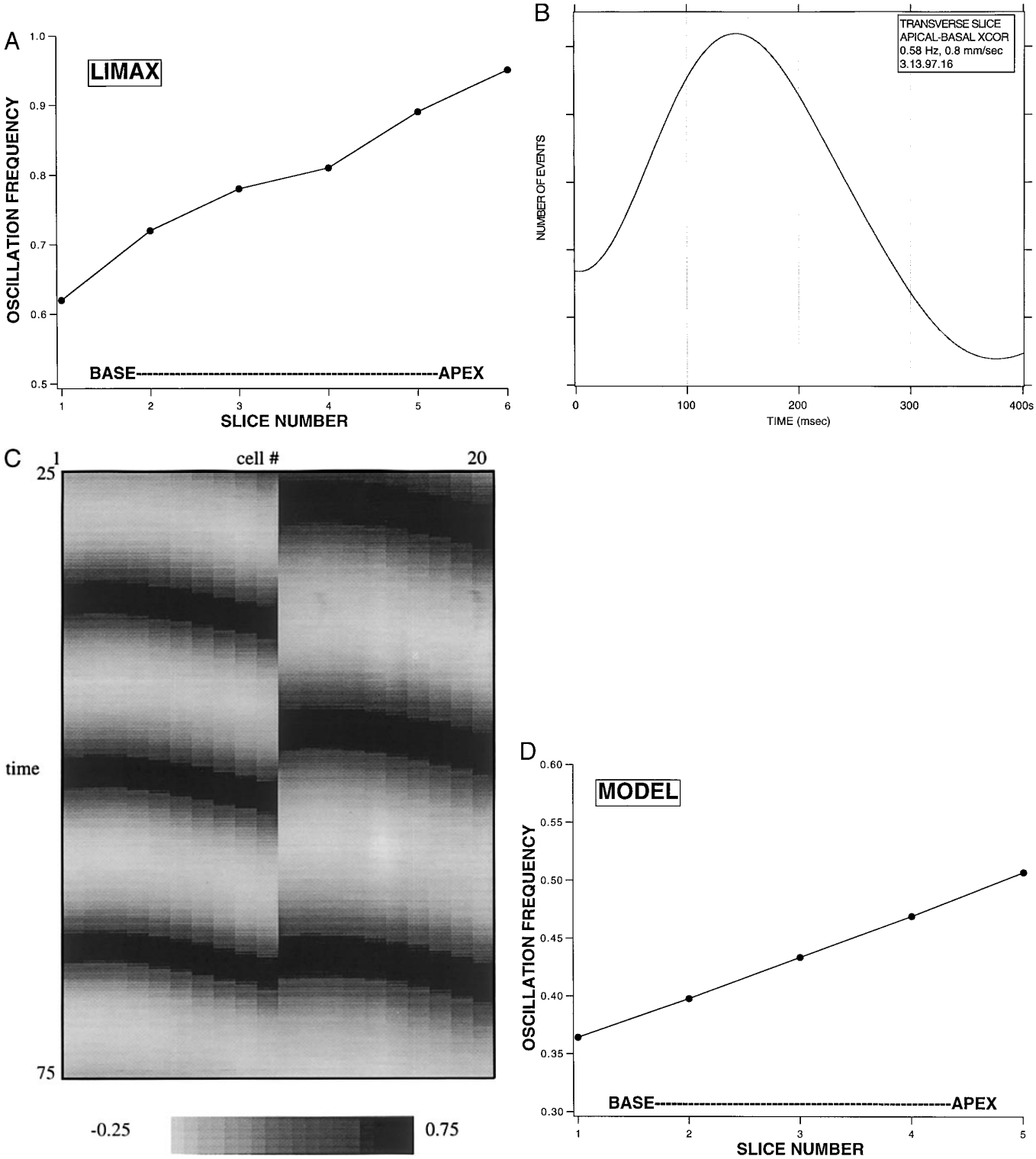

FIG. 4. Oscillations in transverse slices of PC lobes and in transverse slices of the model. *A*: single site measures of the local field potential ocillation in a series of tranverse slices, which vary in their apical-basal position in the PC lobe. Most apical slice has the fastest oscillation. *B*: cross-correlation between apical and basal recordings of the oscillating local field potential taken wthin a single slice. Two recording sites were separated by 110 μm along the apical-basal axis within the slice. Phase lag between the recording sites leads to a non-0 peak in the crosscorrelation, indicating continued wave propagation within the slice. *C*: output of model equations when the apical half of the model (rows 1–10) is disconnected from the basal half (rows 11–20). Apical half (*left*) has a frequency of 0.42 Hz and the basal half (*right*) has a frequency of 0.33 Hz. *D*: output of model after cutting it into 5 equal transverse slices (rows 1–4, 5–8, 9–12, 13–16, and 17–20).

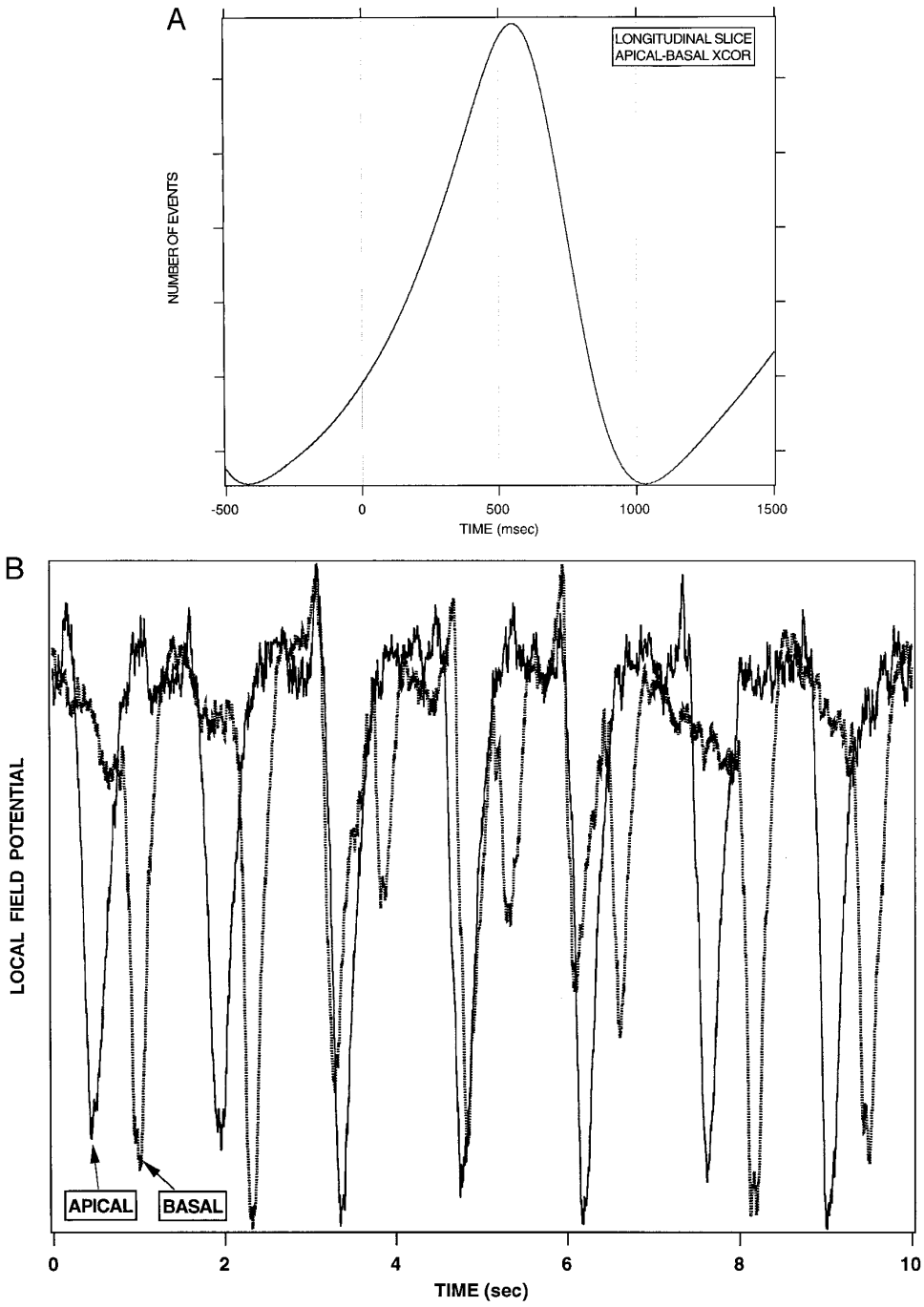

FIG. 5. Oscillations in longitudinal slice of the PC lobe cut along the apical-basal axis. *A*: phase delays between peak activity at the apical and basal recording sites result in a nonzero offset of the cross-correlation between apical and basal recordings, indicating wave propagation. *B*: periods of wave activity are interrupted by rapid transitions to spatially uniform activity, indicated by collapse of the phase gradient in peak activity between apical and basal recording sites.

pletely through the cell layer in the midregion of the intact PC lobe would lead to decorrelation of the apical and basal oscillations. The model, however, predicts that local interactions between the cell and neuropil layers will bridge a cut in the cell layer such that apical and basal recordings remain correlated. The effect of cutting completely through the cell layer in the midregion of the PC lobe on the correlation of the apical and basal recordings is shown in Fig. 6. Records from the apical and basal sites before and after the cut are shown (Fig. 6, *A* and *B*). Interruption of the cell layer did increase the apical-basal latency somewhat and reduced the frequency, but the two sites remain strongly coupled. This result is obtained even when the cut clearly extends through the cell layer into the TM, the cut edges gape open so they are not in contact, and a piece of fine wire is placed in the bottom of the cut to insure its patency.

To investigate further the length scale of the neuropil connections that bridge an interruption in the cell layer, we prepared longitudinal slices, made two cuts through the cell layer ~150 μm apart in the midregion of the slice and then removed the 150-μm region of the cell layer between the cuts (Fig. 7*A*). The recordings at apical and basal sites in the cell body layer before (Fig. 7, *B* and *C*) and after (Fig. 7, *D* and *E*) cell removal indicate that the apical and basal sites remain well coupled in spite of the 150-μm gap in the cell layer. The wave velocity decreased due to cell removal, from 0.8 mm/s precut to 0.5 mm/s postcut.

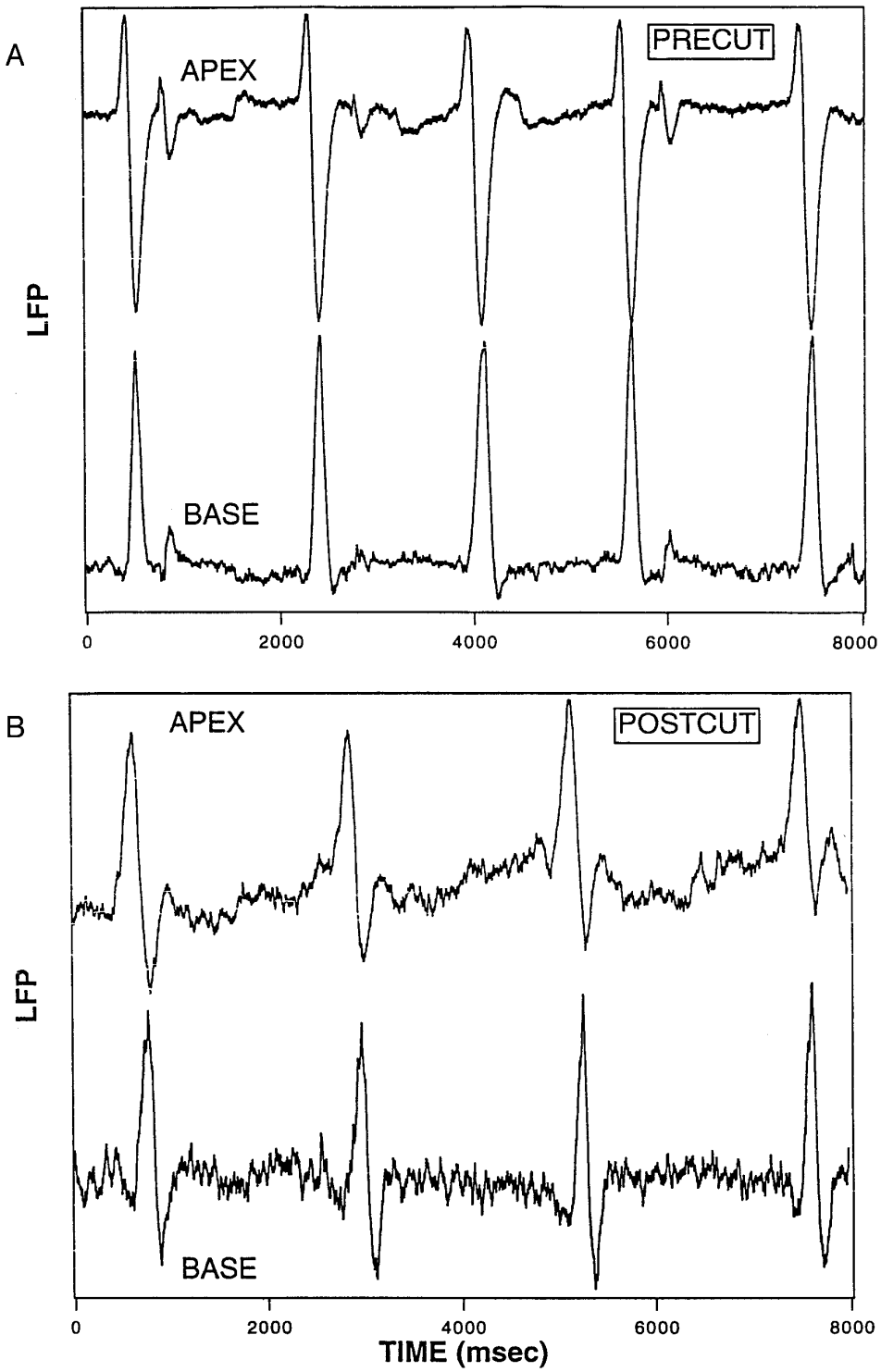

FIG. 6. Cutting completely through the cell layer in the midregion of the PC lobe does not decouple the apical and basal halves. *A*: activity at apical and basal recording sites before cutting the cell layer. *B*: activity at apical and basal recording sites after making a transverse cut completely through the cell layer in the midregion of the PC lobe.

B cells must propagate activity into the neuropil, either directly or indirectly. B cells have neurites running predominately within the cell body layer, whereas NB cells have neurites extending directly into the adjacent neuropil, the TM. Anatomic evidence for B cell neurites extending into the TM was found by localized DiI application (Molecular Probes, No. 383) (Gelperin and Flores 1997) to the TM; on rare occasions, this labeled presumptive B cell somata with multiple neurites, two running in the cell layer and one extending out of the cell layer into the TM (data not shown).

MODEL. Figure 8*A* shows the effect of cutting the B cell layer. The coupling via the NB cells remains. The phase shift increases by ~20% from the uncut preparation. The frequency stays about the same as the uncut preparation.

Activity after cutting neuropil layer

PHYSIOLOGY. To investigate the effect of transecting the neuropil layers on wave propagation, whole desheathed PC lobes were prepared with cuts through the entire neuropil

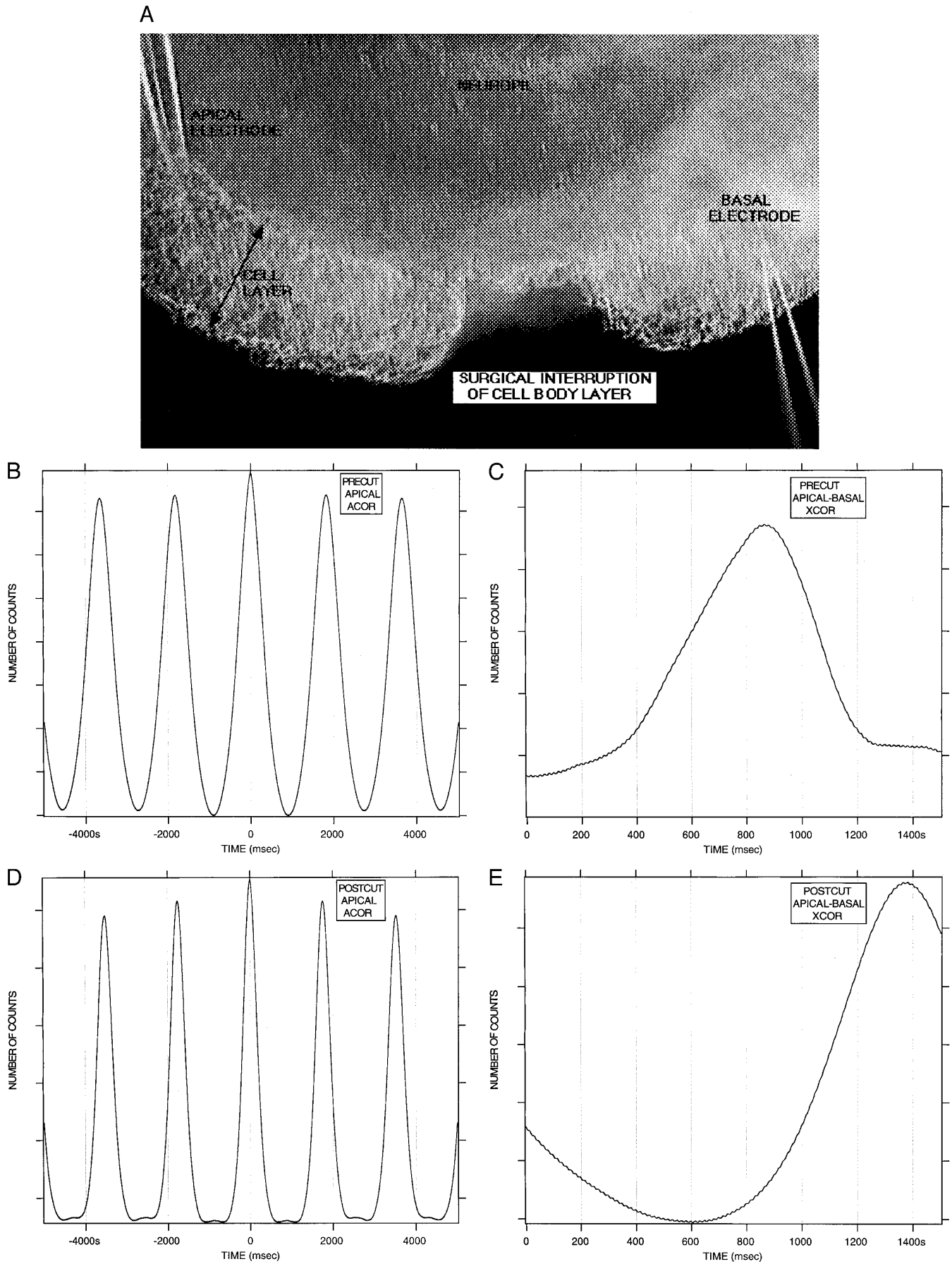
A
APICAL ELECTRODE
NEUROPIL
BASAL ELECTRODE
CELL LAYER
SURGICAL INTERRUPTION OF CELL BODY LAYER
B
PRECUT APICAL ACOR
NUMBER OF COUNTS
-4000s
-2000
0
2000
4000
TIME (msec)
C
PRECUT APICAL-BASAL XCOR
NUMBER OF COUNTS
0
200
400
600
800
1000
1200
1400s
TIME (msec)
D
POSTCUT APICAL ACOR
NUMBER OF COUNTS
-4000s
-2000
0
2000
4000
TIME (msec)
E
POSTCUT APICAL-BASAL XCOR
NUMBER OF COUNTS
0
200
400
600
800
1000
1200
1400s
TIME (msec)

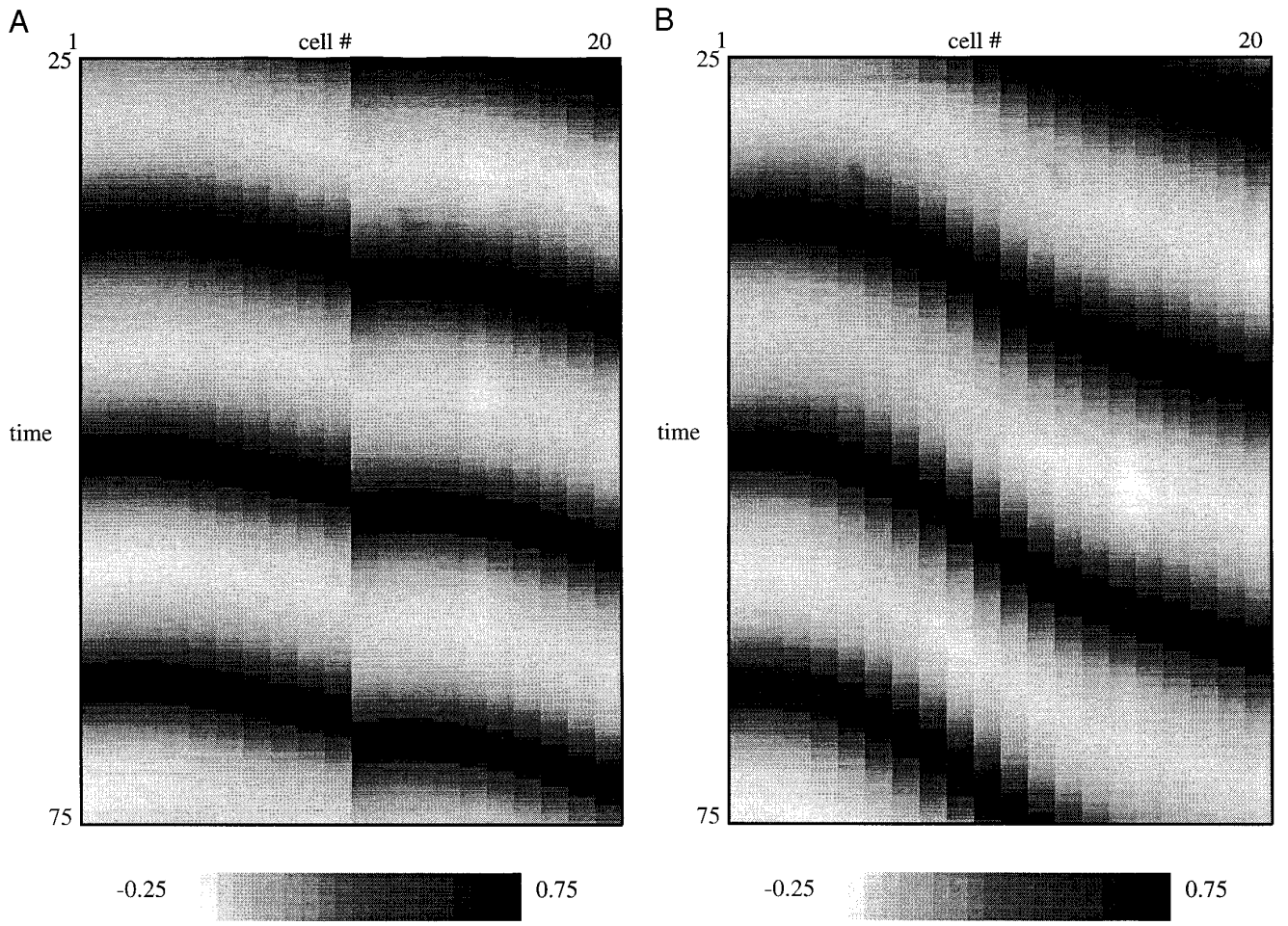

FIG. 8. Effects on model output of cutting through either the burster (B) cell layer or the nonbursting (NB) cell layer. *A*: model output after transecting the B cell layer by decoupling B cells in row 10 from B cells in row 11. *B*: model output after transecting the NB cell layer by decoupling NB cells in row 10 from NB cells in row 11. Gradient more than doubles suggesting that B cell coupling extends farther than nearest neighbor.

and LFP recordings obtained from apical and basal sites in the cell layer. Cross-correlograms showed that activity at the two sites remained tightly coupled in lobes with the neuropil layer completely transected (data not shown).

MODEL. In the model, there is a much more dramatic change after disconnecting row 10 from row 11 in the NB cell layer. The two ends remain phaselocked, but the phase gradient more than doubles (Fig. 8*B*). This suggests that the local B cell coupling extends beyond the nearest neighbors that we have used in the present model. The frequency also is decreased by a small amount.

Activity in isolated cell layer

PHYSIOLOGY. The entire cell layer can be isolated from the neuropil by cutting all neurites at the junction of the TM and cell layer. A cell layer preparation made in this way still oscillates (cf. Fig. 3*B* in Gelperin et al. 1993). Two site recordings of the LFP in the isolated cell layer show that the isolated cell layer makes waves (data not shown).

MODEL. We model this by eliminating the B cell-NB cell interactions. The result is that the waves remain tightly coupled. There is an increase in the gradient but the frequency remains essentially unchanged.

Effects of odor stimulation

PHYSIOLOGY. As shown in previous work (Gervais et al. 1996; Kleinfeld et al. 1994), the activation of olfactory receptors by natural odorants applied to the sensory epithelium of a nose-brain preparation causes a transient collapse of the apical-basal gradient of activity. This effect can be mimicked by shock of the olfactory nerve, which also decreases the apical-basal phase gradient (data not shown).

MODEL. As seen in Fig. 9*A*, the phase gradient collapses upon stimulation and quickly recovers after stimulation. We also show the ''potential'' of two cells separated by half a

FIG. 7. Removal of a 150-μm-wide section of cell layer from the midregion of a 200-μm-thick longitudinal slice of the PC lobe does not decouple the apical and basal regions. *A*: photomicrograph of a longitudinal slice of the PC lobe with a 150-μm-wide segment of the cell body layer removed. *B*: autocorrelation of the apical recording before cell removal. *C*: cross-correlation between apical and basal recordings before cell removal. *D*: autocorrelation of the apical recording after cell removal. *E*: cross-correlation between apical and basal recording after cell removal.

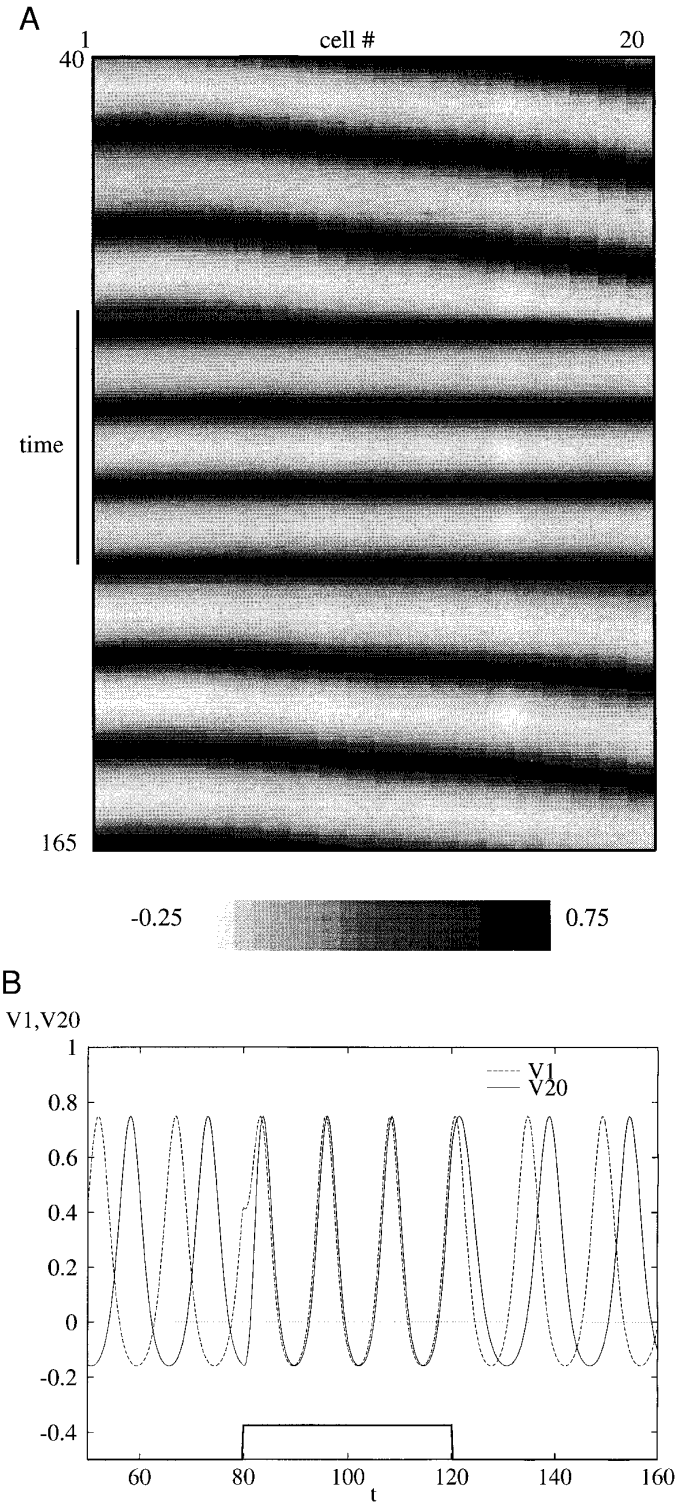

FIG. 9. Afferent input causes the phase gradient of model activity to collapse. *A*: wave activity of the model is suppressed during the period of odor stimulation indicated by the vertical black bar. *B*: pseudopotentials of 2 cells separated by half a lobe length along the apical-basal axis also show the collapse of the phase gradient induced by odor stimulation.

lobe length along the apical-basal axis (Fig. 9*B*). When the stimulus comes on, the oscillators quickly synchronize because the activation of all the NB cells results in global coupling between the B cells.

Effects of reduced chloride saline

PHYSIOLOGY. The direction of wave propagation in the intact PC lobe can be reversed by the application of saline containing 24.2 versus 79.4 mM Cl^- in standard saline, with gluconate replacing Cl. Imaging of wave activity under these conditions shows transient periods during which the basal peak precedes the apical peak; compare Fig. 19 in Kleinfeld et al. (1994).

MODEL. We model lowered chloride by a change in sign of ξ, which means that coupling now decreases frequency instead of increasing it as in normal saline. To justify this on biological grounds, we considered a simple model for a neural oscillator, the Morris-Lecar system (Morris and Lecar 1981). We chose parameters for this model so that it oscillates spontaneously. We then used averaging methods to compute the interaction function for two such weakly coupled oscillating cells and varied the reversal potential of the coupling synapse. By starting with a reversal potential close to that of chloride (-65 mV) and increasing this to -50 mV to mimic the effects of decreasing extracellular chloride, we found that the interaction function can switch sign near zero phase while maintaining a positive slope. Thus our simple model for the effect of reduced chloride is not completely arbitrary.

It is easy to understand these results when we look at two cells coupled together with asymmetric wrights. Think of *cell 1* as apical and *cell 2* as basal. The equations are

$$\theta_1' = \omega_0 + A_1 H(\theta_2 - \theta_1)$$

$$\theta_2' = \omega_0 + A_2 H(\theta_1 - \theta_2)$$

Let $\phi = \theta_2 - \theta_1$ be the phase difference between the apical and basal ends. $\phi < 0$ is the usual wave because the waves propagates from the apical to the basal end; $\phi > 0$ is a reversed wave where the basal end leads and the apical end lags. Then

$$\phi' = A_2 H(-\phi) - A_1 H(\phi)$$

A phaselocked solution is an equilibrium solution to this equation, so phaselocking occurs at the value of where $A_2 H(-\phi) = A_1 H(\phi)$. Furthermore the change in frequency is just

$$\Delta\omega = A_1 H(\phi) = A_2 H(-\phi)$$

Figure 10, *A* and *B*, shows the results of this calculation for $A_1 > A_2$ and either the normal case, $\xi < 0$ or the reversed case $\xi > 0$. Clearly in the normal case, $\phi < 0$ and $\Delta\omega > 0$ so the apical end leads and the frequency is increased relative to the uncoupled case. In the low chloride case, $\xi > 0$ so the apical end lags and the frequency is decreased. In Fig. 10*C* we show the reversal of the phase gradient as varies from -0.1 to 0.02. For $= -0.1$, the phase of excitation in row 20 (basal end) lags row 1 (apical end), whereas with $\xi = 0.02$, the phase relations of basal and apical ends reverse.

DISCUSSION

The model that we have presented here is simple and yet quite general. Because we do not know the details of the synaptic interactions nor the biophysical properties of the cells, we must create models that do not depend on these

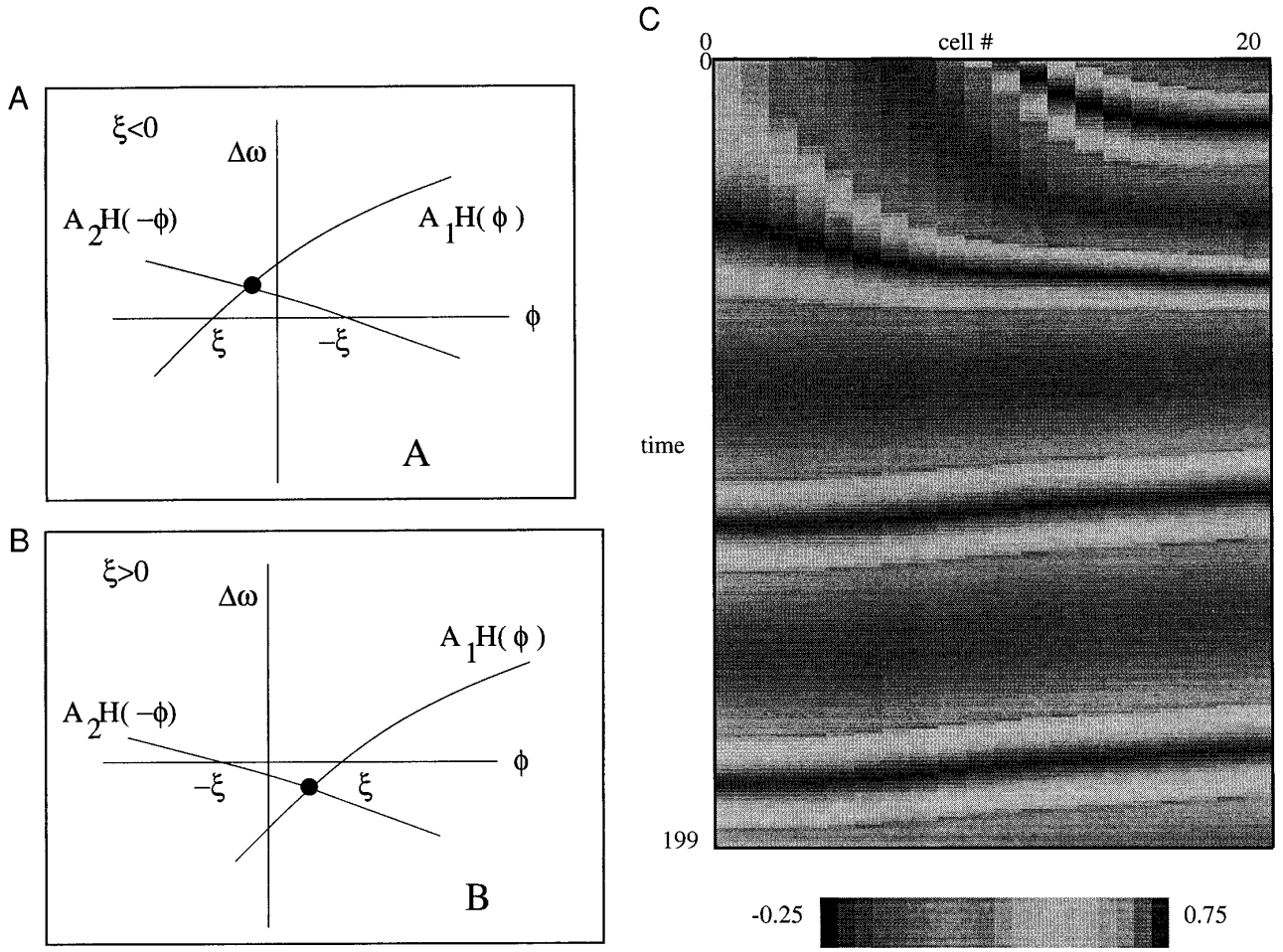

FIG. 10. Reversal of phase gradient of activity in model PC lobe as effects of cell coupling are modified from decreasing to increasing the frequency of coupled cells. *A*: equilibrium solution to the coupling equations when $\xi < 0$. *B*: equilibrium solution to the coupling equations when $\xi > 0$. *C*: change in the phase gradient when the coupling term ξ in *Eq. 4* is varied from -0.1 to 0.02 and the result plotted for the subsequent 200 time steps.

details. Phase models have been successful in suggesting and explaining experiments for the lamprey swim central pattern generator (Williams et al. 1990). The present model, although abstract, provides a framework for our study of the phase gradient in the PC lobe. It captures most of the qualitative properties of the waves as well as more complicated phenomena such as the dependence of the wave direction on chloride concentration.

There are a variety of mechanisms that can give rise to propagating waves of activity in networks of coupled neurons. The best know mechanism is one in which a region of excited tissue excites neighboring sites, and this results in a wave of activity propagating outward from the site of the initial excitation. Such waves are observed in disinhibited cortical slices (Golomb and Amitai 1997; Traub et al. 1993) as well as in the thalamic slice preparation (Kim et al. 1995). Waves that originate from this recruitment mechanism travel in either direction and are stopped by a cut transverse to the propagation direction. Phase waves, set up by a gradient in phase among a group of coupled oscillating neurons, are another common mechanism for the production of waves. This mechanism has been suggested to occur in the lamprey motor system (Williams et al. 1990). Phase waves are not blocked by transverse cuts; although the two sides of the cut may become desynchronized, both remain active. Furthermore, waves of this type tend to travel in one direction only. These properties have suggested to us that the waves in the *Limax* PC lobe are likely to arise due to a phase gradient in a population of intrinsically oscillating cells. Thus the waves observed in the PC lobe appear to be quite different from waves elicited in the slice preparations.

Odor stimulation causes the PC wave to collapse and implies that the neurons within the lobe are synchronized tightly. This synchronization also occurs concurrent with the appearance of doublets in the local field potential (cf. Fig. 5*B*). It is tempting to suggest some connection between the doublets observed in the LFP and those seen in hippocampus during synchronization (Traub et al. 1996, 1997; Whittington et al. 1995). In Traub's models, the principle carriers of the rhythm are a population of inhibitory interneurons. However, Traub's simulations and subsequent mathematical analysis (Ermentrout and Kopell 1997), show that the doublets in the inhibitory interneurons are a result of synaptic bombardment by local and distant excitatory pyramidal cells. In the PC lobe, by the second peak of the LFP doublet, the phase gradient becomes apparent once again. Thus we be-

lieve that the mechanism for the doublets and their role in synchronization of cells in the PC lobe is different from that in the hippocampus.

Fukai (1996) has developed a model for interactions between mammalian olfactory bulb and cortex. He has two populations of excitatory and inhibitory neurons that are connected locally by nearest neighbors. There is additionally a global coupling term with weights that are determined associatively. He reduces this to a phase model by averaging. The resulting phase model generates waves but because his coupling is isotropic and homogeneous, there are waves that either emanate from the center or begin at the edges and collide in the middle. He excludes the global associative term in his averaged model and thus there is never synchrony.

The *Limax* PC lobe is the major central site of odor processing, analogous to the olfactory bulb of vertebrates (Ache 1991; Chase and Tolloczko 1993). Activity with spatial or temporal dynamics similar to that of the PC lobe has been observed in central olfactory structures of invertebrates (Delaney and Kleinfeld 1995; Gervais et al. 1996; Heinbockel et al. 1998; Kleinfeld et al. 1994; Laurent et al. 1996; Mellon et al. 1992; Wu et al. 1995; Kimura et al. 1998a) and numerous vertebrate species (Adrian 1942; Barrie et al. 1996; Delaney and Hall 1995; Gerard and Young 1937; Tank et al. 1994). Coherent network oscillations also are found in visual cortex (Gray and Diprisco 1997) and in other cortical and subcortical systems in the mammalian brain (reviews in Basar and Bullock 1992; Singer and Gray 1995), including humans (Llinas and Ribary 1993; Ribary et al. 1991; Tallon-Baudry et al. 1997). Oscillatory field potential activity is thought to reflect close temporal correlations in neuron activity which facilitate feature detection or synaptic plasticity.

Rhythmically active groups of coupled inhibitory interneurons have been shown to underlie the PC oscillation (Delaney and Kleinfeld 1995; Kleinfeld et al. 1994) and coherent gamma-frequency activity in hippocampus (Traub et al. 1997; Whittington et al. 1995). Both structures are implicated in mnemonic functions. The PC lobe's involvement in odor learning is suggested by the observation of learning-specific labelling of PC cells by Lucifer yellow (Kimura et al. 1998b) and the finding that inhibition of nitric oxide synthase blocks odor learning in vivo (Teyke 1996) and the PC oscillation in vitro (Gelperin 1994). In hippocampus, recent evidence suggests that the disruptive effects of sedatives and anesthetics on gamma oscillations may underlie their cognitive effects (Whittington et al. 1996). By contrast picrotoxin-induced desynchronization of coherent activity in the honeybee, antennal lobe had no effect on odor-sucrose conditioning of the proboscis extension reflex (Stopfer et al. 1997).

We thank J. J. Hopfield for comments on the manuscript.

Portions of this study were supported by National Science Foundation Grant DMS-9626728 and National Institute of Mental Health Grants MH-47150 to B. Ermentrout and MH-56090 to A. Gelperin.

Address for reprint requests: A. Gelperin, Room 1C464, Bell Laboratories, 600 Mountain Ave., Murray Hill, NJ 07974.
E-mail: CNSAG@bell-labs.com

Received 25 August 1997; accepted in final form 27 January 1998.

REFERENCES

ACHE, B. W. Phylogeny of smell and taste. In: *Smell and Taste in Health and Disease*, edited by T. V. Getchell, R. L. Doty, L. M. Bartoshuk, and J. B. Snow. New York: Raven Press, 1991, p. 3–18.

ADRIAN, E. D. Olfactory reactions in the brain of the hedgehog. *J. Physiol. (Lond.)* 100: 459–473, 1942.

BARRIE, J. M., FREEMAN, W. J., AND LENHART, M. D. Spatiotemporal analysis of prepyriform, visual, auditory, and somesthetic surface EEGs in trained rabbits. *J. Neurophysiol.* 76: 520–539, 1996.

BASAR, E. AND BULLOCK, T. H. *Induced Rhythms in the Brain.* Boston, MA: Birkhauser, 1992.

CHASE, R. AND TOLLOCZKO, B. Tracing neural pathways in snail olfaction: from the tip of the tentacles to the brain and beyond. *Microsc. Res. Tech.* 24: 214–230, 1993.

DELANEY, K. R., GELPERIN, A., FEE, M. S., FLORES, J. A., GERVAIS, R., TANK, D. W., AND KLEINFELD, D. Waves and stimulus-modulated dynamics in an oscillating olfactory network. *Proc. Natl. Acad. Sci. USA* 91: 669–673, 1994.

DELANEY, K. R. AND HALL, J. B. An in vitro preparation of frog nose and brain for the study of odour-evoked oscillatory activity. *J. Neurosci. Methods* 68: 193–202, 1995.

DELANEY, K. R. AND KLEINFELD, D. Spatio-temporal dynamics of oscillatory activity in frog olfactory bulb. *Soc. Neurosci. Abstr.* 21: 1182, 1995.

ERMENTROUT, G. B. AND KOPELL, N. Multiple pulse interactions and averaging in systems of coupled neural oscillators. *J. Math. Biol.* 29: 195–217, 1991.

ERMENTROUT, G. B. AND KOPELL, N. Inhibition-produced patterning in chains of coupled nonlinear oscillators. *SIAM J. Appl. Math.* 54: 478–507, 1994.

ERMENTROUT, B. AND KOPELL, N. Fine structure of neural spiking and synchronization in the presence of conduction delays. *Proc. Natl. Acad. Sci. USA* 95: 1259–1264, 1998.

FUKAI, T. Bulbocortical interplay in olfactory information processing via synchronous oscillations. *Biol. Cybern.* 74: 309–317, 1996.

GELPERIN, A. Nitric oxide mediates network oscillations of olfactory interneurons in a terrestrial mollusc. *Nature* 369: 61–63, 1994.

GELPERIN, A. AND FLORES, J. Vital staining from dye-coated microprobes identifies new olfactory interneurons for optical and electrical recording. *J. Neurosci. Methods* 72: 97–108, 1997.

GELPERIN, A., KLEINFELD, D., DENK, W., AND COOKE, I.R.C. Oscillations and gaseous oxides in invertebrate olfaction. *J Neurobiol.* 30: 110–122, 1996.

GELPERIN, A., RHINES, L., FLORES, J. AND TANK, D. Coherent network oscillations by olfactory interneurons: modulation by endogenous amines. *J. Neurophysiol.* 69: 1930–1939, 1993.

GELPERIN, A. AND TANK, D. W. Odor-modulated collective network oscillations of olfactory interneurons in a terrestrial mollusc. *Nature* 345: 437–440, 1990.

GERARD, R. W. AND YOUNG, J. Z. Electrical activity of the central nervous system of the frog. *Proc. R. Soc. Lond. B Biol. Sci.* 122: 343–352, 1937.

GERVAIS, R., KLEINFELD, D., DELANEY, K. R., AND GELPERIN, A. Central and reflex neuronal responses elicited ,by odor in a terrestrial mollusc. *J. Neurophysiol.* 76: 1327–1339, 1996.

GOLOMB, D. AND AMITAI, Y. Propagating neuronal discharges in neocortical slices: computational and experimental study. *J. Neurophysiol.* 78: 1199–1211, 1997.

GOLOMB, D., WANG, X. J., AND RINZEL, J. Propagation of spindle waves in a thalamic slice model. *J. Neurophysiol.* 75: 750–769, 1996.

GRAY, C. M. Synchronous oscillations in neuronal systems: mechanisms and functions. *J. Comput. Neurosci.* 1: 11–38, 1994.

GRAY, C. M. AND DIPRISCO, G. V. Stimulus dependent neuronal oscillations and local synchronization in striate cortex of the alert cat. *J. Neurosci.* 17: 3239–3253, 1997.

GRAY, C. M. AND MCCORMICK, D. A. Chattering cells: superficial pyramidal neurons contributing to the generation of synchronous oscillations in the visual cortex. *Science* 274: 109–113, 1996.

HANSEL, D., MATO, G., AND MEUNIER, C. Synchrony in excitatory neural networks. *Neural Comput.* 5: 307–337, 1995.

HEINBOCKEL, T., KLOPPENBURG, P., AND HILDEBRAND, J. G. Pheromone-evoked potentials and oscillations in the antennal lobes of the sphinx moth *Manduca sexta*. *J. Comp. Physiol.* [*A*] In press.

HOPFIELD, J. J. Pattern recognition computation using action potential timing for stimulus representation. *Nature* 376: 33–36, 1995.

KAWAHARA, S., TODA, S., SUZUKI, Y., WATANABE, S., AND KIRINO, Y. Comparative study on neural oscillation in the procerebrum of the terrestrial slugs *Incilaria bilineata* and *Limax marginatus*. *J. Exp. Biol.* 200: 1851–1861, 1997.

KIM, U., BAL, T., AND MCCORMICK, D. A. Spindle waves are propagating

synchronized oscillations in the ferret LGNd in vitro. *J. Neurophysiol.* 74: 1301–1323, 1995.

KIMURA, T., SUZUKI, H., KONO, E., AND SEKIGUCHI, T. Mapping of interneurons which contribute to food aversion conditioning in the slug brain. *Learn. Mem.* 4: 376–388, 1998a.

KIMURA, T., TODA, S., SEKIGUCHI, T., AND KIRINO, Y. Behavioral modulation induced by food odor aversion conditioning, and its influence on the olfactory responses of an oscillatory brain network in the slug, *Limax marginatus. Learn. Mem.* 4: 365–375, 1998b.

KLEINFELD, D., DELANEY, K. R., FEE, M. S., FLORES, J. A., TANK, D. W., AND GELPERIN, A. Dynamics of propagating waves in the olfactory network of a terrestrial mollusc: an electrical and optical study. *J. Neurophysiol.* 72: 1402–1419, 1994.

KOPELL, N. AND ERMENTROUT, G. B. Coupled oscillators and the design of central pattern generators. *Math. Biosci.* 90: 87–109, 1988.

LAURENT, G., WEHR, M., MACLEOD, K., STOPFER, M., LEITCH, B., AND DAVIDOWITZ, H. Dynamic encoding of odors with oscillating neuronal assemblies in the locust brain. *Biol. Bull.* 191: 70–75, 1996.

LLINAS, R. AND RIBARY, U. Coherent 40-Hz oscillation characterizes dream state in humans. *Proc. Natl. Acad. Sci. USA* 90: 2078–2081, 1993.

MELLON, D., SANDEMAN, D. C., AND SANDEMAN, R. E. Characterization of oscillatory olfactory interneurons in the protocerebrum of the crayfish. *J. Exp. Biol.* 167: 15–38, 1992.

MORRIS, C. AND LECAR, H. Voltage oscillations in the barnacle giant muscle fiber. *Biophys. J.* 35: 193–213, 1981.

RATTE, S. AND CHASE, R. Morphology of interneurons in the procerebrum of the snail *Helix aspersa*. *J. Comp. Neurol.* 384: 359–372, 1997.

RIBARY, U., JOANNIDES, A. A., SINGH, K. D., HASSON, R., BOLTON, J.P.R., LADO, F., MOGILNER, A., AND LLINAS, R. Magnetic field tomography of coherent thalamocortical 40 Hz oscillations in humans. *Proc. Natl. Acad. Sci USA* 88: 11037–11041, 1991.

SINGER, W. AND GRAY, C. M. Visual feature integration and the temporal correlation hypothesis. *Annu. Rev. Neurosci.* 18: 555–586, 1995.

STOPFER, M., BHAGAVAN, S., SMITH, B. H., AND LAURENT, G. Impaired odour discrimination on desynchronization of odour-encoding neural assemblies. *Nature* 390: 70–74, 1997.

TALLON-BAUDRY, C., BERTRAND, O., DELPUECH, C., AND PERNIER, J. Oscillatory γ-band (30–70 Hz) activity induced by a visual search task in humans. *J. Neurosci.* 17: 722–734, 1997.

TANK, D. W., GELPERIN, A., AND KLEINFELD, D. Odors, oscillations, and waves: does it all compute? *Science* 265: 1819–1820, 1994.

TEYKE, T. Nitric oxide, but not serotonin, is involved in acquisition of food-attraction conditioning in the snail *Helix pomatia*. *Neurosci. Lett.* 206: 29–32, 1996.

TRAUB, R. D., JEFFREYS, J.G.R., AND MILES, R. Analysis of propagation of disinhibition-induced after-discharges along the guinea pig hippocampal slice in vitro. *J. Physiol. (Lond.)* 472: 267–287, 1993.

TRAUB, R. D., JEFFERYS, J.G.R., AND WHITTINGTON, M. A. Simulation of gamma rhythms in networks of interneurons and pyramidal cells. *J. Comput. Neurosci.* 4: 141–150, 1997.

TRAUB, R. D., WHITTINGTON, M. A., STANFORD, I. M., AND JEFFERYS, J.G.R. A mechanism for generation of long-range synchronous fast oscillations in the cortex. *Nature* 383: 621–624, 1996.

VAN VREESWIJK, C., ABBOTT, L. F., AND ERMENTROUT, G. B. When inhibition, not excitation synchronizes neural firing. *J. Comp. Neurosci.* 1: 313–321, 1994.

WATANABE, S., KAWAHARA, S., AND KIRINO, Y. Morphological chracterization of the bursting and nonbursting neurons in the olfactory center of the terrestrial slug *Limax marginatus*. *J. Exp. Biol.* 201: 925–930, 1998.

WEHR, M. AND LAURENT, G. Odour encoding by temporal sequences of firing in oscillating neural assemblies. *Nature* 384: 162–166, 1996.

WHITTINGTON, M. A., JEFFREYS, J.G.R., AND TRAUB, R. D. Effects of intravenous anesthetic agents on fast inhibitory oscillations in the rat hippocampus in vitro. *Br. J. Pharmacol.* 118: 1977–1986, 1996.

WHITTINGTON, M. A., TRAUB, R. D., AND JEFFERYS, J.G.R. Synchronized oscillations in interneuron networks driven by metabotropic glutamate receptor activation. *Nature* 373: 612–615, 1995.

WILLIAMS, T., SIGVARDT, K., KOPELL, N., ERMENTROUT, B., AND REMLER, M. Forcing of coupled nonlinear oscillators: studies of intersegmental coordination of the lamprey locomotor central pattern generator. *J. Neurophysiol.* 64: 862–871, 1990.

WU, J. Y., WU, C. H., GUAN, L., AND COHEN, A. H. Local field potential in the antennal lobe of the Antheraea moth (*A. pernyi*): pheromone related oscillations? *Soc. Neurosci. Abstr.* 21: 134, 1995.

ZAITSEVA, O. V. Structural organisation of the tentacular sensory system in land pulmonates. In: *Simpler Nervous Systems*, edited by D. A. Sakharov and W. Winlow. New York: Manchester University Press, 1991, p. 238–257.

ZS.-NAGY, I. AND SAKHAROV, D. A. The fine structure of the procerebrum of pulmonate molluscs, *Helix* and *Limax*. *Tissue Cell* 2: 399–411, 1970.